Effects of the Inhomogeneity of the Time Resolving CMOS Single-Photon Avalanche Diode Array on Time-gated Raman Spectroscopy

Ilkka Nissinen, Jan Nissinen and Juha Kostamovaara
Circuits and Systems Research Unit
University of Oulu
Oulu, Finland
firstname.lastaname@ee.oulu.fi

***Abstract*—The effects of the inhomogeneity of a time resolving CMOS single-photon avalanche diode array on the fluorescence-suppressed, time-gated, Raman spectroscopy device was experimentally studied here. Raman spectroscopy device using a 532 nm pulsed laser and a single time resolving single-photon avalanche diode (SPAD) with a micro step motor was developed to study these effects. A single SPAD with a step motor allows us to test the performance which could be achieved with an ideal line detector without any nonlinearities and inhomogeneities because the same SPAD and time interval measurement unit is used in every spectral point. Additionally, the single element can be replaced by a SPAD array with an on-chip time-to-digital converter (TDC) to make comparison measurements to clarify the effects of inhomogeneity. These comparison measurements were made by using an array of 256 elements with an on-chip 100 ps TDC and showed that the deterioration of Raman spectra is larger when fluorescence lifetimes and levels are shorter and higher, respectively.**

Keywords—Single-photon counting; Geiger detector;

I. INTRODUCTION

Raman spectroscopy is a well-known optical spectroscopic technique that gives a large amount of information about the molecular structure and chemical environment of the sample. It has been used in many applications in the field of biology, chemistry and food, pharma and oil industries [1-6]. The conventional Raman spectroscopy is based on a CW laser and a CCD detector, and unfortunately both the Raman scattered and fluorescence induced photons are collected. Thus, the Raman spectrum of the samples with a high fluorescence background is difficult or even impossible to resolve. This is a major issue why the conventional Raman spectroscopy is not widely used in some otherwise potential applications [7].

Fortunately, Raman and fluorescence photons have different time responses. Raman photons are scattered immediately when the sample is illuminated by the laser whereas fluorescence photons experience an exponentially decaying time response. Thus, the photons can be separated in the time domain, for example by using short (much shorter than fluorescence lifetime), intensive laser pulses (not CW laser) to illuminate the sample and by recording the sample response only during these short pulses [8,9]. Using the "time gating", the amount of fluorescence photons can be dramatically reduced if the fluorescence lifetime is much larger than the time gate and a short laser pulse used, as shown in Fig. 1.

This kind of "time gating" technique has been applied in previous work [8-10]. Unfortunately, since these techniques utilize a high-speed optical shutter based on a Kerr cell and a mode-locked laser with spectrograph and ICCD (intensified CCD), they are sophisticated, large and expensive systems that are not suitable for emerging on-site applications, for example. To overcome these problems, the CCDs and ICCDs should be replaced with a detector that can be time-gated and which could be fabricated as an array and does not need any cooling, for example.

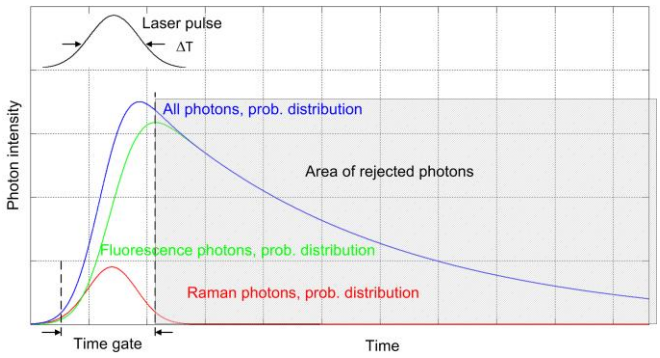

Fig. 1. Principle of time gating.

Single photon avalanche diodes (SPAD) and SPAD arrays have been fabricated by using commercial CMOS technologies for approximately 10 years [11]. SPAD is a p-n junction which is biased with a reverse bias voltage above its breakdown voltage and is thus operating in the so-called Geiger mode. Nowadays, there are different technologies with different line widths available to manufacture SPAD arrays for applications such as time resolved fluorescence measurement [12], time-of-light laser range finding [13] and positron emission tomography [14,15], for example. At the beginning of this decade we presented the idea of using of a time-gated SPAD as the detector of a Raman spectroscopy device to suppress the

high fluorescence background [16]. The SPAD is well-suited for Raman spectroscopy because it can detect single photons and thus a weak Raman scattering can be detected and additionally, the time gating can be constructed in the same die with a SPAD quite easily compared to ICCDs and CCDs without any cooling. Several other groups have also presented SPADs and SPAD arrays for time-gated Raman spectroscopy [17-20]. As has been shown, SPADs are suitable for array structures where the time gating electronics with a timing resolution of hundreds of picoseconds can be realized in the same die [19,20]. To achieve adequate fluorescence suppression with a high fluorescence background having lifetimes of several nanoseconds, a time gate width of hundreds of picoseconds or less is required. However, when designing larger and larger arrays with a ~100 ps accuracy, the complexity of the design is increasing and thus the derivation of Raman spectrum is complicated by the inevitable inhomogeneities of the SPAD array and time gating electronics. This makes designing an array with a high quality and homogeneity a very demanding task from the point of view of the timing skew and variation of time gating, for example.

In this work we present the measurement results in which the effect of non-homogeneities and nonlinearities of a time-gated 256 SPADs line detector are compared to the results achieved without these errors. The reference Raman spectrometer is based on the use of a single SPAD detector which is moved with a micro step motor to achieve the required spectral range. An off-chip time-to-digital converter (TDC) is used to store the times of arrival of each photon scattered from the sample, as shown in Fig. 2 a). The illumination is based on a 532 nm pulsed laser (Teem Photonics) and a grating is used to spread the photons with different wavelength to the SPAD at a different position. The times of arrival of photons (STOPs signals in Fig. 2 b)) can be recorded in relation to the excited laser pulses.

This device makes it possible to measure the ultimate performance in time-gated Raman spectroscopy because a single SPAD and TDC are not affected by the noise and the inhomogeneities of time gating through the whole line detector since one and only SPAD and one time interval measurement unit are being used at every spectral point. In addition, as the times of arrival of each photon are recorded with a high resolution (24 ps), a proper time gating can be realized in post-processing based e.g. on Matlab code to derive the Raman spectrum from the histogram files. The disadvantage of this system is that the derivation of the whole spectrum takes more time than in a system utilizing a wider line detector. In the above system, the single element detector can be replaced by a time-gated 256-element SPAD line detector to perform the comparison measurements.

In what follows we first in Chapter II describe the structure of the time-gated Raman spectroscopy system. In Chapter III we give some measurement results with reference samples and a sample known to have a high fluorescence background (olive and sesame seed oil). Chapter IV gives the conclusions of the work.

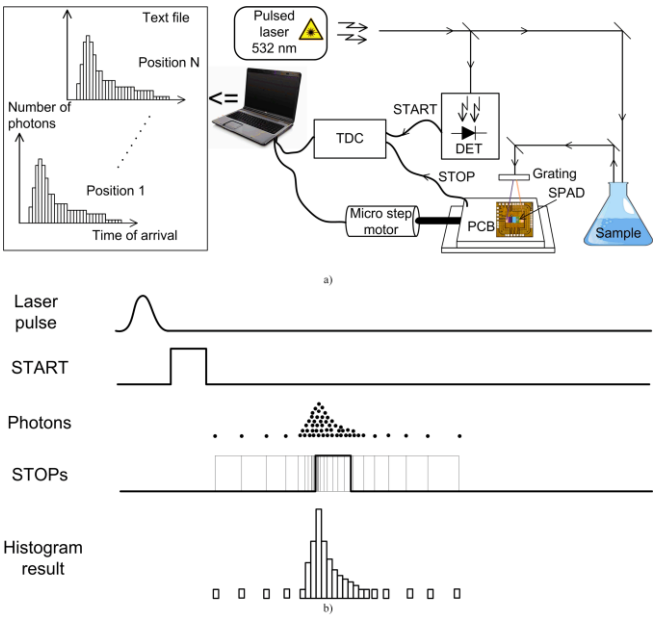

Fig. 2. a) Block and b) timing diagram of the time-gated Raman spectrometer.

II. Time-gated Raman Spectroscopy using a CMOS SPAD and a Time-to-Digital Converter

The time-gated SPAD-based Raman spectroscopy setup presented here is based on a pulsed laser with a sub-nanosecond optical pulse and a passively quenched SPAD detector. The proposed Raman spectroscopy setup is shown in Fig. 3 where it has been divided in three parts: (1) laser, (2) sampling optics and (3) spectrograph and detector. The purpose of the sampling optics is firstly to deliver the optical pulse from the laser to the sample and secondly to collect photons from the sample and deliver them to the spectrograph and filter out the laser wavelength. Photons having different wavelengths are spread spatially by the grating to the detector. Spectral information is then formed based on the location of the detector, which can be adjusted by the micro step motor.

A pulsed laser from Teem Photonics has been used as a laser source. The pulse energy of 1.2 µJ with a pulsing rate of 4 kHz can be delivered to the sample. The width (FWHM) of the optical pulse is 500 ps. The optical pulse from the laser is directed to the sample using a fiber with a coupler. The fiber collimator has been used to collimate the beam when it exits the fiber. Because coaxial excitation has been utilized, the same objective is also used as a collection optic which directs photons from the sample having higher wavelengths than laser through the dichroid (D in Fig. 3). In addition there is a mirror to rotate the beam 90° towards the input slit.

The spectrometer is based on a grating spectrograph and SPAD detector with a micro step motor (Thorlabs). The scattered photons from the sample are directed to the input slit with a width of 50 µm and a holographic grating (G in Fig. 3) after which the beam goes through the focusing lens to arrive in the SPAD detector. The SPAD detector of an active area diameter of 10 µm and designed in a 0.35 µm HVCMOS technology is used here. The SPAD detector chip is placed on a

test card which is moved by the micro step motor (Thorlabs) along the spectral axis so that the wavelength information of the scattered photons can be solved. Whenever a photon is detected by the SPAD detector, it generates a logic level timing mark for a time interval measurement unit (ORTEC TAC with data analyzer) (TDC in Fig. 2) which produces the time distribution of the detected photons with the resolution of ~24 ps. Because a free running laser is used, the synchronizing signal (START in Fig. 2) to the TDC is generated from the small portion of an optical pulse through a dichroid (D in Fig. 3) by an optical detector (DET in Fig. 2 and Fig. 3). The whole measurement setup is controlled by a laptop with Labview.

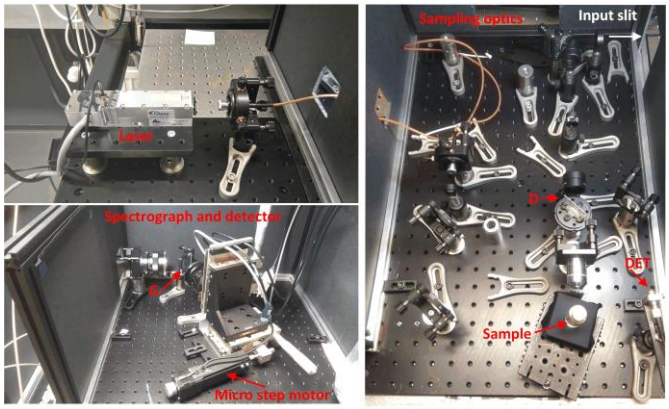

Fig. 3. Used Raman spectroscopy setup.

III. Measurement Results

As presented above, the aim of this work was construct a time-gated Raman spectroscopy device utilizing a single CMOS SPAD and the TDC with an accurate micro step motor to achieve a uniform response over the whole spectral range from the point of view of the detector and time-to-digital converter. This system was used as a reference system which can give Raman results which could be achieved by means of an ideal detector array. At the beginning, the performance of the constructed time-gated Raman spectroscopy system in the wavelength domain was measured by means of the calibration measurements with known reference samples. After that high fluorescence and short lifetime samples were used to make a comparison between the single element device and a time-gated 256 SPADs line detector.

A step motor was used to move the single element over the whole spectral range and the accuracy of it was better than that of the grating limiting the spectral resolution (~10 cm^{-1} corresponds to ~50 μm).

A. Spectral Resolution Measurement

In order to gain adequate step size for the step motor, the spectral resolution measurement of the Raman spectroscopy system was carried out with a known reference sample, the mixture of a toluene and an acetonitrile with the ratio of 1:1 whose Raman spectrum is shown in Fig. 4 [21]. The Raman peak at the 786.5 cm^{-1} shown in Fig. 4 was used as a "spectral" impulse stimulus after it was located by using coarse sweep. The step size of 5 μm of a micro step motor (half of the diameter of the SPAD) was used to solve the spectral resolution i.e. the spectral bandwidth of our whole Raman spectroscopy device. The step size of 5 μm corresponds to the spectral resolution of 0.9 cm^{-1}, which is better than that of the grating and the pulsed laser used. Fig. 5 a) shows the Raman peak at 786.5 cm^{-1} measured by our system with the step size of 5 μm. The spectral bandwidth of the system was derived to be 14 cm^{-1} (793 cm^{-1} – 779 cm^{-1}) from Fig. 5 a) corresponding to the step size of 78 μm. The step size of 50 μm was chosen to be adequate for Raman measurements, as demonstrated in Fig. 5 b), where the same Raman peak at 786.5 cm^{-1} was measured by using the step size of 50 μm giving a similar curve. Unless otherwise stated, this step size was used in all measurements. Note that as the diameter of the SPAD is 10 μm, the step size of 50 μm is leaving empty points between adjacent steps, but the measurement is five times faster.

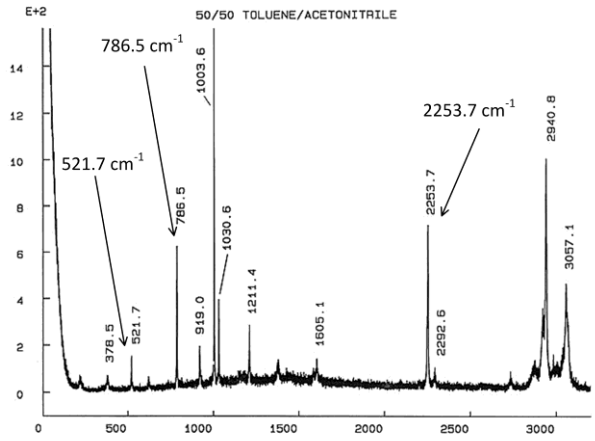

Fig. 4. Raman spectra of reference sample the mixture of a toluene and an acetonitrile.

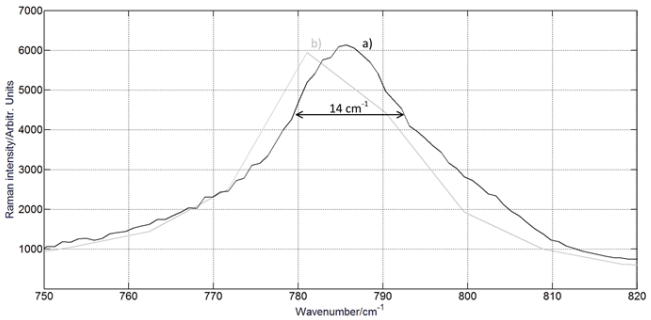

Fig. 5. Raman peak at 786.5 cm^{-1} of the mixture of a toluene and an acetonitrile measured by using a) the step size of 5 μm and b) the step size of 50 μm.

B. Calibration Measurements n

To calibrate the wavenumber domain, i.e. the position of the step motor, known reference sample, the same mixture as above was used. The wavelength calibration was made by measuring the Raman spectrum of the mixture by using our time-gated Raman spectroscopy device over the wavenumber

range from approximately 500 cm^{-1} to 2 400 cm^{-1}. Two peaks (521.7 cm^{-1} and 2 253.7 cm^{-1} from Fig. 4)) were used to set the positions of the step motor, and the compensation curve was derived in order to achieve the best possible fitting. The calibrated Raman spectrum of the mixture of a toluene and an acetonitrile measured by our device is shown in Fig. 6. All the Raman peaks can be found at the right places within the resolution of 9 cm^{-1} except the Raman peak at the 1 030.6 cm^{-1} shown in Fig. 4. This peak is merged to the higher peak at 1 003.6 cm^{-1} because of the limited spectral bandwidth of our system, but the small peak at 2 292.6 cm^{-1} shown in Fig. 4 (2 301 cm^{-1} in Fig. 6)) beside the peak at the 2 253.7 cm^{-1} (2 262 cm^{-1} in Fig. 6) can be derived by our system as the separation of these peaks is approximately 40 cm^{-1}.

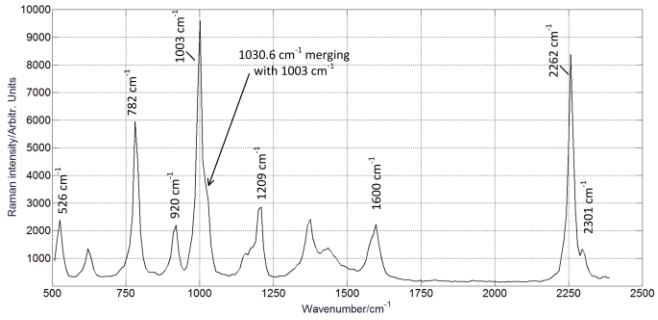

Fig. 6. Raman spectrum of the mixture of a toluene and an acetonitrile measured by our device.

The intensity calibration was made by using a continuous wave light source (Ando AQ-4303B light source) which was measured by the presented time-gated Raman spectroscopy system and by an optical spectrum analyzer (Ando AQ-6315A) over the wavelength range from 550 nm to 638 nm corresponding to wavenumber range from 628 cm^{-1} to 3 124 cm^{-1} in Raman spectroscopy. The intensity calibration curve derived from those results is shown in Fig. 7. The waves are caused by the interference of the layers above the SPAD surface relating to the fabrication process of CMOS technology.

C. Raman Test Measurement with a Known Sample

Olive oil was used as a high fluorescence sample, which was measured by the above time-gated Raman spectroscopy device with a single SPAD and TDC and micro step motor to test the accuracy in the wavelength domain and the fluorescence suppression available. The background fluorescence is suppressed by using the time of arrival of photon histograms and summing the photons within the laser pulse, and additionally, the residual fluorescence level is further suppressed by subtracting the residual level estimated by the collection of the fluorescence photon after a laser pulse [22]. The most important Raman peaks of cooking oils are located within the spectral range from 800 cm^{-1} to 1 800 cm^{-1} and are at the wavenumbers of 1 268 cm^{-1}, 1 302 cm^{-1}, 1 442 cm^{-1}, 1 660 cm^{-1} and 1 750 cm^{-1} [23]. The compensated Raman spectra of an olive oil sample derived by the time gate of approximately 700 ps and 20 ns are shown in Fig. 8 with a solid line and dotted line, respectively, to show the functionality of the fluorescence suppression. As can be seen in Fig. 8, all the Raman peaks can be found at the correct places within the spectral resolution of our device, and the high fluorescence background is dramatically suppressed with a time gate of 700 ps.

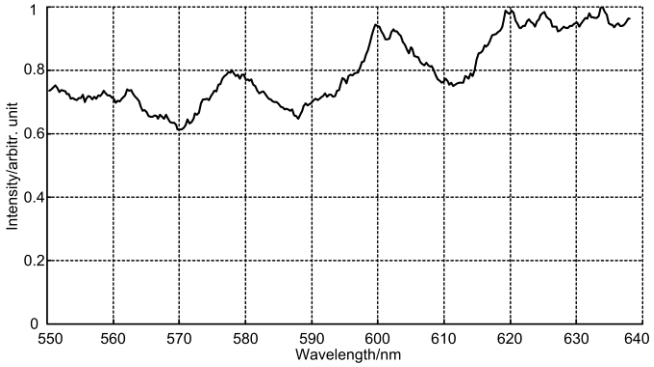

Fig. 7. The intensity calibration curve of time-gated Raman spectroscopy.

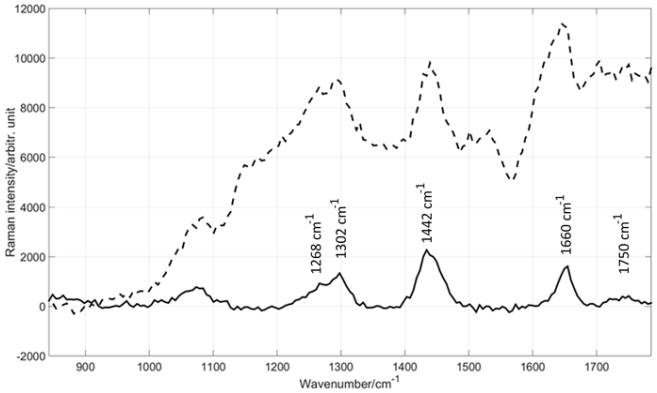

Fig. 8. Raman spectrum of olive oil with time gate of 20 ns (dotted line) and time gate of 700 ps (solid line).

D. Comparison Measurements

As mentioned above, using a single detector and a step motor, the errors caused by the inhomogeneity of the line detector can be avoided, yet at the expense of a longer measurement time. To clarify the effect of the inhomogeneity of the line detector, olive and sesame seed oils were measured by using both detectors, a single element with an off-chip TDC and 256 elements with an on-chip TDC. The 256 SPADs array consists of a 256-channel on-chip TDC having a resolution of 100 ps and a dynamic range of approximately 700 ps and thus the similar measurements as performed by using a single element and the off-chip TDC could be made. Therefore, Raman spectra measured by using the 256 SPADs array with the on-chip TDC were derived by summing the photons within the whole dynamic range of 700 ps to derive comparable results. Sesame seed oil has approximately the same fluorescence lifetime (~2 ns) as olive oil, but the fluorescence level is one decade higher than that of olive oil. Raman spectra of olive and sesame seed oils measured by the Raman spectroscopy system based on a single element (black) and 256 elements (grey) are shown in Fig. 9 and 10, respectively. As can be seen in both figures, the spectrum measured by a single

element has a better signal-to-noise ratio compared to that measured by the 256 SPADs. The increased noise is caused by the inhomogeneities of elements and time gating electronics in a line detector. The deterioration of the spectrum is larger when sesame seed oil is measured, because it has a higher fluorescence background compared to olive oil. Comparison measurements showed that the complexity of the array will increase the effect of inhomogeneity of SPADs and their time gating on Raman spectrum. To increase the number of SPADs in a line detector more, the time gating of the SPADs has to be designed carefully to achieve the best possible performance.

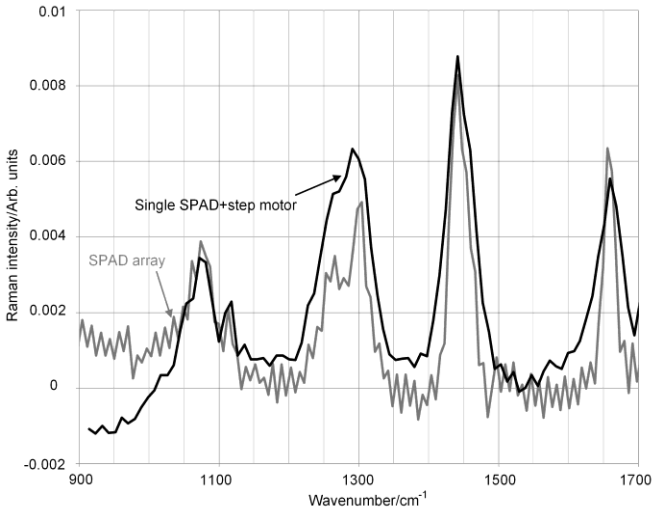

Fig. 9. Raman spectra of olive oil measured by using a single SPAD with micro step motor and 256 SPADs.

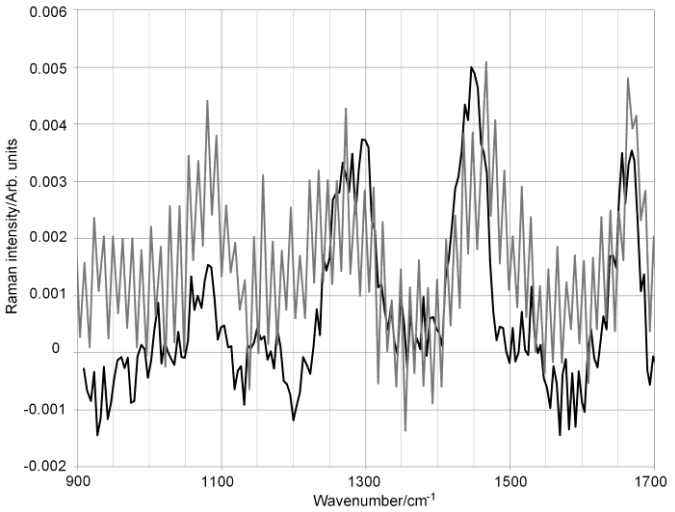

Fig. 10. Raman spectra of sesame seed oil measured by using a single SPAD with micro step motor and 256 SPADs.

IV. Conclusions

A time-gated Raman spectroscopy system based on a grating, a pulsed laser (FWHM = 500 ps) and a time resolving CMOS single-photon avalanche diode with a micro step motor have been presented in order to measure the "ideal" reference accuracy for a time-gated multi-element line detector with an on-chip TDC. Some comparison measurements were made to study the effect of the inhomogeneity of a time-gated multi-element line detector on the Raman spectrum. Measurements with 256 SPADs line detector with an on-chip TDC showed that the SNR deterioration due to non-homogeneities is noticeable. The use of detector arrays speed up the measurement system but, the array should be designed carefully to achieve an adequate performance.

Acknowledgment

The authors also wish to acknowledge the contribution of Lauri Kurki of TimeGate Instruments Ltd. (Oulu, Finland) in developing the optomechanics of the Raman spectrometer measurement system.

References

[1] E.B. Hanlon, R. Manoharan, T-W. Koo, K.E. Shafer, J.T. Motz, M. Fitzmaurice, J.R. Kramer I. Itzkan, R.R. Dasari and M.S. Feld. "Prospects for in vivo Raman spectroscopy". Physics in Medicine and Biology. 2000. 45(2): R1-R59.

[2] Nancy L. Jestel. "Process Raman Spectroscopy". In: K. A, Bakeev, editors. Process Analytical Technology: Spectroscopic Tools and Implementation Strategies for the Chemical and Pharmaceutical Industries. Chichester, UK: John Wiley and Sons, 2010. Chap. 7, Pp. 195-244.

[3] O. Khalil. "Spectroscopic and Clinical Aspects of Noninvasive Glucose Measurements". Clinical Chemistry. 1999. 45(2): 165–177.

[4] D. Tuschel. "Raman Spectroscopy of Oil Shale". Spectroscopy Solutions for Materials Analysis. 2013. 28(3): 20-27.

[5] T. Vankeirsbilck, A. Vercauteren, W. Baeyens, G. Van der Weken, F. Verpoort, G. Vergote and J.P. Remon. "Applications of Raman spectroscopy in pharmaceutical analysis". Journal of Trends in analytical chemistry. 2002. (21)12: 869-877.

[6] Y. Li and J. S. Church. "Raman spectroscopy in the analysis of food and pharmaceutical nanomaterials". Journal of Food and Drug Analysis. 2014. 22(1): 29-48.

[7] M. L'Heureux. "Analysis of the State of the Art: Raman Spectroscopy". Spectroscopy. 2015. 30(6).

[8] P. Matousek, M. Towrie, C. Ma, W.M. Kwok, D. Phillips, W.T. Toner, and A.W. Parker. "Fluorescence suppression in resonance Raman spectroscopy using a high-performance picosecond Kerr gate". Journal of Raman Spectroscopy. 2001. 32(12): 983-988.

[9] R.P. Van Duyne, D.L. Jeanmaire, and D.F. Shriver. "Mode-Locked Laser Raman Spectroscopy-A New Technique for the Rejection of Interfering Background Luminescence Signals". Analytical Chemistry. 1974. 46(2): 213-222.

[10] E.V. Efremov, J.B. Buijs, C. Gooijer, and F. Ariese. "Fluorescence Rejection in Resonance Raman Spectroscopy Using a Picosecond-Gated Intensified Charge-Coupled Device Camera". Applied Spectroscopy. 2007. 61(6): 571-578.

[11] A. Rochas, M. Cani, B. Furrer, P. A. Besse, R. S. Popovic, G. Ribordy and N. Gisin. "Single photon detector fabricated in a complementary metal-oxide-semiconductor high voltage technology". Review of Scientific Instruments. 2003. 74(7): 3263-3270.

[12] D. Mosconi, D. Stoppa, L. Pancheri, L. Gonzo and A. Simoni. "CMOS Single-Photon Avalanche Diode Array for Time-Resolved Fluorescence Detection". Paper presented at: IEEE European Solid-State Circuits Conference (ESSCIRC'06), Montreux, Switzerland; September 18-22, 2006.

[13] C.Niclass, A.Rochas, P.-A.Besse and E.Charbon. "Designand characterization of a CMOS 3-D image sensor based on single photon avalanche diodes". IEEE Journal of Solid-State Circuits. 2005. 40(9): 1847–1854.

[14] L. H. C. Braga, L. Pancheri, L. Gasparini, M. Perenzoni, R. Walker, R. K. Henderson and D. Stoppa. "A CMOS mini-SiPM detector with in-pixel data compression for PET applications". Paper presented at: IEEE Nuclear Science Symposium and Medical Imaging Conference, Valencia, Italy; October 23-29, 2011.

[15] L. H. C. Braga, L. Gasparini, L. Grant, R. K. Henderson, N. Massari, M. Perenzoni, D. Stoppa and R. Walker. "A Fully Digital 8 x 16 SiPM Array for PET Applications With Per-Pixel TDC and Real-Time Energy Output". IEEE Journal of Solid-State Circuits. 2014. 49(1): 301–314.

[16] I. Nissinen, J. Nissinen, A-K Länsman, L. Hallman, A. Kilpelä, J. Kostamovaara, M. Kögler, M. Aikio, J. Tenhunen. "A sub-ns time-gated CMOS single photon avalanche diode detector for Raman spectroscopy". Paper presented at: IEEE European Solid-State Device Research Conference (ESSDERC'11), Helsinki, Finland; September 12-16, 2011.

[17] Y. Maruyama, J. Blacksberg and E. Charbon. "A 1024x8, 700-ps Time-Gated SPAD Line Sensor for Planetary Surface Exploration With Laser Raman Spectroscopy and LIBS". IEEE Journal of Solid-State Circuits. 2014. 49(1): 179-189.

[18] N. Krstajic, R. Walker, J. Levitt, S. P. Poland, D. Li, S. Ameer-Beg and R.K. Henderson. "A 256 x 8 SPAD Line Sensor for Time Resolved Fluorescence and Raman Sensing". Paper presented at: IEEE European Solid-State Circuits Conference (ESSCIRC'14), Venezia, Italy; September 22-26, 2014.

[19] I. Nissinen, J. Nissinen, P. Keränen, A-K. Länsman, J. Holma and J. Kostamovaara." A 2x(4)x128 Multi-time-gated SPAD Line Detector for Pulsed Raman Spectroscopy". IEEE Journal of Sensors. 2015. 15(3): 1358-1365.

[20] I. Nissinen, J. Nissinen, J. Holma and J. Kostamovaara. " A 4 x 128 SPAD array with a 78-ps 512-channel TDC for time-gated pulsed Raman spectroscopy". Springer Science and Business Media, Analog Integrated Circuits and Signal Processing. 2015. 84(3): 353-362.

[21] McCreery Group. "Standard Spectra" http://www.chem.ualberta.ca/~mccreery/ramanmaterials.html [accessed February 4 2016]

[22] J. Kostamovaara, J. Tenhunen, M. Kögler, I. Nissinen, J. Nissinen and P. Keränen. "Fluorescence suppression in Raman spectroscopy using a time-gated CMOS SPAD". Optics Express. 2013. 21(25): 31632-31645.

[23] Process Instruments. "Edible Oils: Safflower, Peanut, Olive, Corn, Canola, Vegetable" http://www.process-instruments-inc.com/pdf/PI_Raman_Cooking_Oils.pdf [accessed December 18 2015]